

New Dopamine/Hexamolybdate Nanostructures for Oral Drug Delivery

Mariam Radhi Kadhim¹, Ahmed Al-Yasari^{2*}, Ihsan Mahdi Shaheed³, Stephen Barton³

¹ Department of Chemistry, College of Science, University of Kerbala, Al-Ferahe, Kerbala, Iraq

² School of Chemistry, University of East Anglia, Norwich Research Park, Norwich, NR7 4TJ, UK

³ School of Life Sciences, Pharmacy and Chemistry, Kingston University London, Kingston-Upon-Thames KT1 1LQ, Surrey, U.K.

Abstract

The synthesis of new 3D nanostructures via the self-assembly of organic-inorganic hybrids from polyoxometalate (POM) Lindqvist-type hexamolybdate with dopamine has been explored. The as-prepared nanostructures were investigated for use as nanocarriers for the drug temozolomide (TMZ), which is used in chemotherapy. The release behavior of TMZ from the nanocarrier at different pHs was studied. The surface morphologies, topographies, and sizes of the nanostructures, as well as their chemical compositions and identities, were investigated via HPLC, FTIR, XRD, SEM, and XPS. The nanocarriers showed an interesting pH-dependent release behavior, indicating the potential for their use in drug delivery systems.

1. Introduction

Brain tumors such as glioblastoma, despite comprising only 2% of all adult cancer diagnoses, are among the most debilitating of such malignant diseases.^{1,2} Temozolomide (TMZ) (3,4-dihydro-3-methyl-4-oxoimidazo-[5,1-d]-as-tetrazine-8-carboxamide TZ) is an imidazotetrazine derivative alkylating drug developed in the 1980s through rational drug design by the UK Cancer Research Campaign. It is used to treat primary brain tumors, especially glioblastoma multiforme (GBM).^{3,4} TMZ was approved by the FDA for use as an oral capsule on August 11, 1999, and for use in intravenous form on February 27, 2009.¹ TMZ is a prodrug of imidazotetrazine that needs to be hydrolyzed nonenzymatically *in vivo* at physiological pH in order to alkylate adenine/guanine residues. This process damages DNA through cycles of unsuccessful repairing, ultimately leading to cell death.⁵ TMZ is a first-line

Received: 07/01/2025

Accepted: 24/02/2025

Published: 31/08/2025

Keywords: Polyoxometalates (POMs), Dopamine (DA), Temozolomide (TMZ), 3D Nanostructures, Drug Delivery.



drug for GBM treatment, although it has a short half-life in the body and GBM cells show resistance. Therefore, high doses and repeated administration of TMZ are needed, which leads to significant side effects; hence, its efficiency is limited. For this reason, new controlled release strategies for TMZ are needed to maintain therapeutic doses for extended periods, and also to overcome the above limitations. Thus, nanomedicine can be envisaged as a promising approach to the therapy of brain tumors with TMZ by building new nanostructures with varied and superior properties as nanocarriers.

Along with other building blocks, polyoxometalates (POMs), which are highly negatively charged metal oxygen nanoclusters whose sizes and shapes are amenable to control, have received considerable attention as suitable inorganic building blocks for drug delivery systems owing to their potential to increase biocompatibility, enable the selective recognition of biological targets, and modify the bioactivity and cytotoxicity of drugs.^{6–11} In recent years, many pioneering studies have reported the synthesis of the hierarchical nanostructure of dopamine and POMs for the oral delivery of certain drugs.^{12–14} However, the majority of such studies have focused mainly on Keggin, Anderson and Dawson POMs combined with bioactive components such as dopamine to fabricate 3D multifunctional nanostructures.^{15–17} Lindqvist-type hexamolybdate is the most interesting of the polyoxometalates in this regard, and hence has increasingly been investigated due to its potential applications in electronic and photonic devices.^{10,18,19} To the best of our knowledge, the fabrication of 3D nanostructures that combine dopamine and Lindqvist-type hexamolybdate has not previously been reported. This study aims to investigate the formation of nanostructures from POM, particularly Lindqvist-type hexamolybdate, with dopamine (DA) as a nanocarrier for pH-controlled oral drug delivery of TMZ. The as-prepared nanostructures were characterized, and their physical-chemical properties studied.

2. EXPERIMENTAL SECTION

2.1 MATERIALS

Dopamine hydrochloride (DA) was purchased from Thermo Fisher Scientific. Tris (hydroxymethyl) aminomethane (Tris HCL) and phosphate-buffered saline (PBS) were purchased from HiMedia (India). TMZ was obtained from Sigma-Aldrich. Glycine was purchased from Thomas Baker.

2.2 SYNTHESIS OF 3D NANOSTRUCTURES

The nanostructures were formed in a [1:1] ratio of POM-DA. In a typical procedure, solutions of DA (1 mg) and POM (hexamolybdate) (1 mg) were separately prepared in 10 mM Tris HCl solution (pH 10.5, 0.5 ml). The POM solution was immediately added to the DA solution. Within 30 seconds of this addition, the color of the solution visibly changed to red (see Fig. S1). The mixture was aged for 2 h, then centrifuged (5000 rpm, 5 min) and washed three times with water to afford the final product.

2.3 LOADING OF AS-PREPARED NANOSTRUCTURES WITH TMZ

In this study, the model drug was TMZ. A nanopowder of POM-DA was immersed in an aqueous solution of TMZ (0.5 mg/ml, 5ml). The mixture was shaken for 12 h at 25°C, and the resulting product was then washed with pure water three times. In order to remove any unbound drug, the product was then centrifuged at 5000 rpm for 5 min. To determine the proportion of TMZ loaded onto the nano-POM-DA, the amount of unloaded TMZ remaining in the supernatant was determined via HPLC using the chromatographic conditions reported in Table 1.

2.4 RELEASE (IN VITRO) OF LOADED TMZ

TMZ release was achieved by immersing a sample of nanostructures loaded with TMZ (10 mg) under agitation on a shaker plate (500 rpm) in two mediums: an acidic medium (pH 2.8, glycine-HCl buffer solution), and a neutral medium (pH 7.4, phosphate-buffered saline (PBS) solution) over a period of 24 h. The amount of TMZ released in each case was determined by taking aliquots (0.5 ml) of the supernatant at timed intervals. Finally, the amount of TMZ released was measured on the basis of HPLC analysis using the UFLC system of a Shimadzu 20A with a UV detector. The chromatographic conditions were optimized, and which are reported in Table 1.

Table 1. Chromatographic conditions

Column	C18
Mobile phase	Acetonitrile 60:40 Water HPLC
Detector (Wavelength)	328 nm
Flow rate	1.0
Column temperature	37°C
Injection volume	20 µL
Run time	10 min

2.5 CHARACTERIZATION TECHNIQUES

X-ray diffraction (XRD) was performed via a powder X-Ray diffractometer (Siemens model D500) using a Cu filter. Scanning electron microscopy (SEM) (ZEISS model: Sigma VP) was performed under vacuum conditions at a voltage of 25 kV to analyze the size, morphology, and topographical features of the nanostructures. X-ray photoelectron spectroscopy (XPS) (Bes Tek, Germany) was performed with a monochromatic Al K α 1 X-ray source (1486.6 eV) to investigate the chemical composition of the nanostructures.

3. RESULTS AND DISCUSSION

3.1 X-ray DIFFRACTION ANALYSIS

XRD measurements were used to investigate the as-prepared nanostructures. Fig.1-C presents the XRD patterns of the as prepared POM-DA compared to POM (Fig.1-A) and DA (Fig.1-B), where several characteristic Bragg reflections of Lindqvist-type hexamolybdate POMs ($2\theta = 16.5^\circ$), as well as other peaks at $2\theta = 20^\circ$, and 26.5° for DA, could clearly be observed, indicating the successful complexation of DA with POM Lindqvist-type hexamolybdates through strong interactions. Compared to its POM and DA precursors, the POM-DA structure showed broader peaks, which can be attributed the smaller crystalline particle size, confirming the nano-character of the resultant POM-DA composite. These results were also supported by the SEM analysis, which indicated the formation, and illustrated the topography, of the nanostructures, as per Fig. 3. After loading TMZ into the POM-DA nanocomposite, the XRD patterns (Fig.1-D) showed minimal change compared to the POM-DA composite, though boarder peaks were observed.

Fourier-transform infrared (FT-IR) spectra of POM-DA-TMZ nanocomposites in comparison with MTZ and POM, respectively, showed the most characteristic bands of each of the components (POM and TMZ), though with slight shifts at 794, 960, and 1446 cm^{-1} for the POM, indicative of complexation, as shown in Fig. 2.

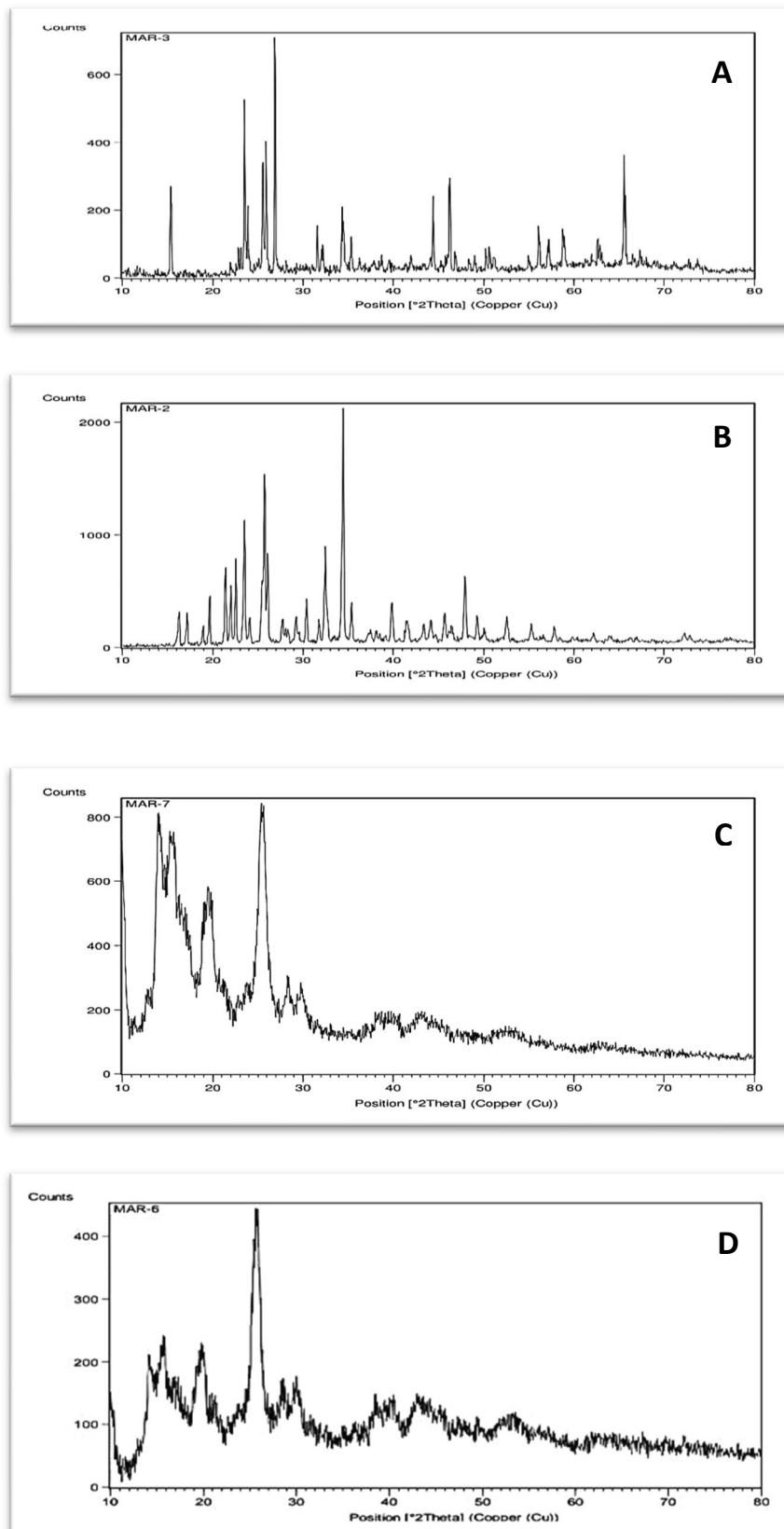


Fig. 1: XRD patterns of (A) POM hexamolybedate; (B) DA; (C) the as-prepared nanostructure prior to loading with TMZ; and (D) the as-prepared nanostructure after loading with TMZ.

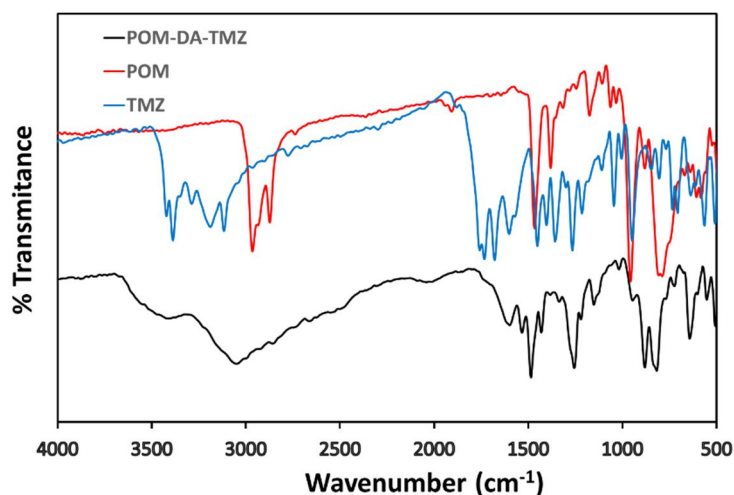


Fig. 2. FTIR spectra of the POM-DA nanocomposite loaded with TMZ (black), POM Lindqvist-type (red), and TMZ (blue).

3.2 SCANNING ELECTRON MICROSCOPY (SEM) ANALYSIS

The morphology of the as-prepared nanostructures of POM-DA before and after loading with TMZ were investigated via SEM. As can be seen from Fig. 3, which shows the SEM micrographs of the POM-DA nanostructure, the nanostructure itself consists of hierarchical microsphere structures with a size of about 1 μm constructed from a multitude of nanopetals of thicknesses ranging from 20 to 40 nm and widths of 300-500 nm. 3D hierarchical structures were formed from the central connection of these nanopetals. The loading of TMZ onto the hierarchical microsphere structures resulted in totally different morphological (shape and size) structures compared to POM-DA. As can be seen from Fig. 4, nanosphere particles with diameters ranging from 20 to 45 nm are formed upon loading with TMZ. These considerable changes in both morphology and size can be attributed to the TMZ loaded onto the surface of POM-DA nanostructure. These findings are consistent with the XRD results, which showed a change to a smaller particle size upon loading of TMZ compared to the naked POM-DA nanostructures.

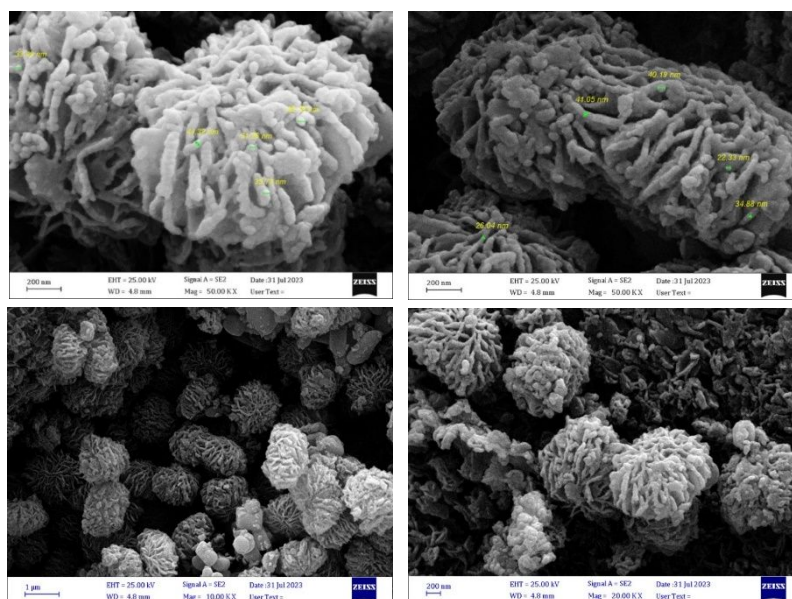


Fig. 3. SEM images of the as-prepared nanostructures prior to loading with TMZ.

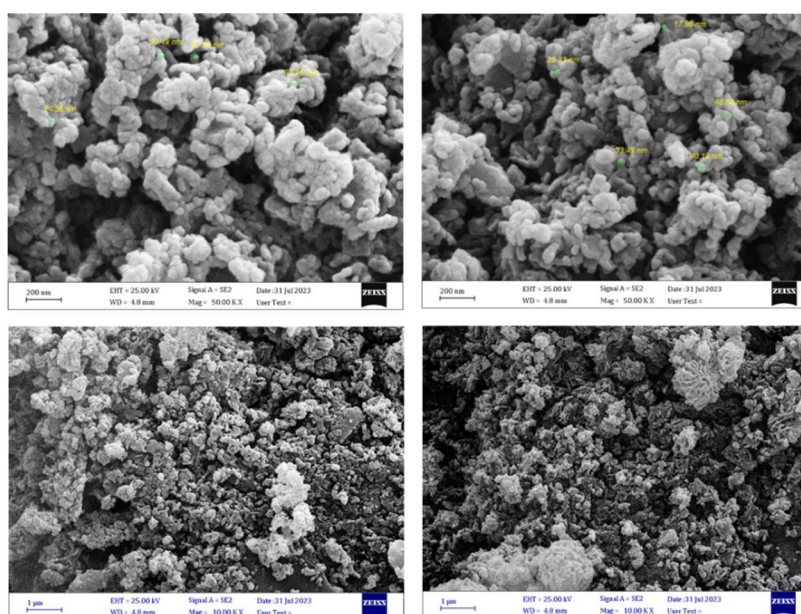


Fig. 4. SEM images of the as-prepared nanostructures after loading with TMZ.

3.3 X-Ray PHOTOELECTRON SPECTRA (XPS)

XPS spectroscopy was performed to identify the elemental composition of the nanocomposites, the results of which are presented in Fig. 5. These confirm the presence of C, N, and Mo, with peaks corresponding to C1s (BE = 289 eV), N1s (BE = 404 eV), and Mo3d_{5/2} (BE = 237 eV). The C1s and the N1s signals can be attributed to the carbon and amido in DA (and TMZ in (b)), while the Mo3d can be attributed to POM Lindqvist-type hexamolybdate. It can clearly be seen that the N1s band comprises two peaks: the first, at 404 eV, can be assigned to alkylamines, whilst the second, at higher binding energy, can be attributed to protonation of the amine groups in DA, confirming the existence of electrostatic interactions between POM and

DA.¹³ XPS results again confirm the successful complexation of DA with POM Lindqvist-type hexamolybdate.

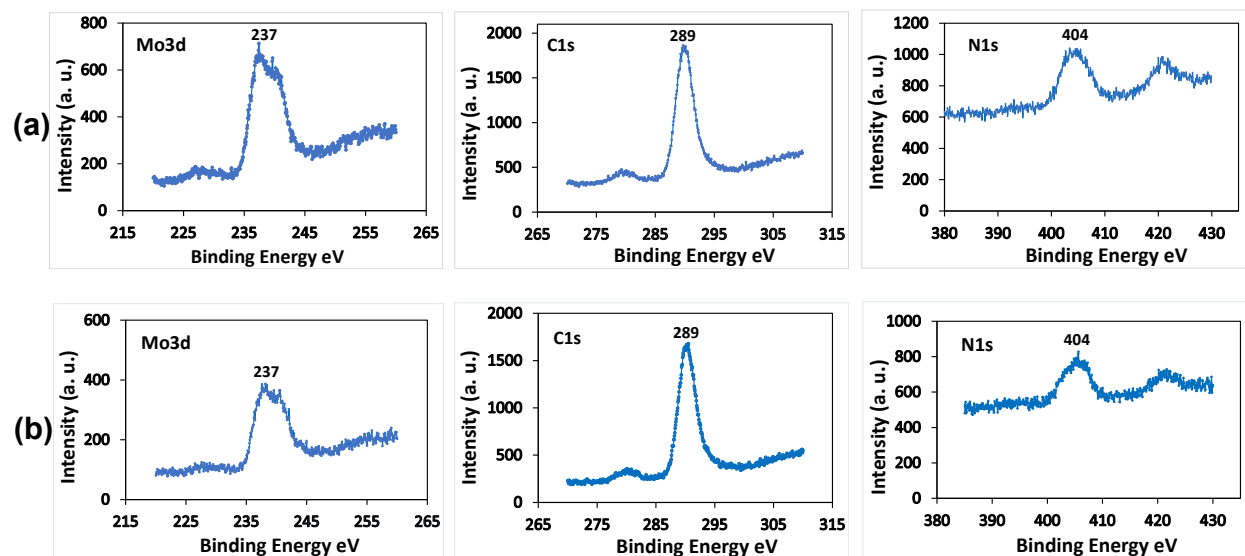


Fig. 5: X-Ray photoelectron spectra of: (a) the as-prepared POM-DA nanostructure prior to loading with TMZ; and (b) the as-prepared POM-DA nanostructure after loading with TMZ.

3.4 RELEASE BEHAVIOR OF TMZ LOADED ONTO AS-PREPARED NANOSTRUCTURES

In this study, the potential of the nanostructures to act as carriers in oral drug delivery were explored by studying the loading and release behavior of TMZ in media of different pHs. Upon loading of TMZ onto the nanostructures, a color change from dark red to red was clearly seen, as shown in Fig. S1, indicating the successful loading of TMZ. The amount of TMZ loaded onto the POM-DA nanostructures was determined via HPLC and was found to be about 38% (by weight), which represents a high loading efficiency. This could be attributed to the large relative surface area (smaller particle size compared to POM-DA prior to loading) of the nanostructures. The utilization of pH changes within the gastrointestinal (GI) tract is one of the most interesting methods in the design of oral delivery protocols for drugs in which two pH changes are chosen, the first mimicking the acidic conditions of the stomach (pH 1–3), and the second the more basic conditions of the intestines (pH 5–8). Fig. 6 shows the release profile of TMZ at pH 2.8 and pH 7.4 over 24 h, from which it can clearly be seen that release was pH dependent. As can be seen from Fig. 6, at pH 7.4 the release of TMZ reaches 97% in 24 h, where in the first four hours the amount released shows a dramatic increase, at up to 90%, which is then followed by a more sustained release over the following 20 h.

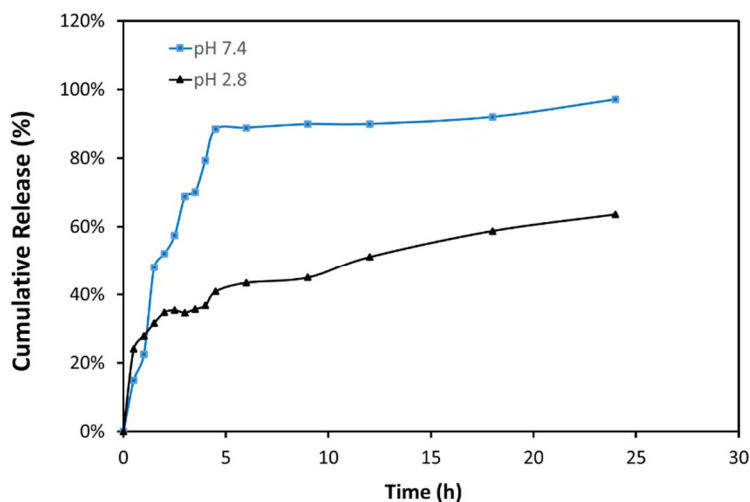


Fig. 6 Release behavior of TMZ loaded onto nanostructures at pH 7.4 (blue) and pH 2.8 (black).

On the other hand, at pH 2.8 the total amount of TMZ released over 24 h was only 64%. An ‘eruption’ release of up to 25% was seen in the first 30 minutes at both pH 7.4 and 2.8, which can be attributed to the physisorption of TMZ onto the dispersed POM-DA nanostructure powder. Compared to the pH 7.4 release profile, the amount of TMZ released at pH 2.8 in the first hour was relatively small, at up to 30%, indicating that the absorption of TMZ is favored at lower pH. Thus, it can clearly be concluded that the release behavior of TMZ from POM-DA nanostructures was pH-responsive. The above results clearly demonstrate the potential use of POM-DA nanostructures as nanocarriers for the oral delivery of TMZ in the therapy for certain cancers.

4. CONCLUSION

In this study, we have successfully prepared new nanocarriers of DA and POM loaded with TMZ (38% loading) via self-assembly as a means of oral drug delivery. The as-prepared nanocarrier form of TMZ was fully characterized via XRD, FTIR, XPS, and SEM. The as-prepared oral form of TMZ showed an excellent pH-dependent release of TMZ, where the release rate at pH 7.4 was considerably faster than at pH 2.8. Further work is requested to investigate these nanostructures for other drug systems and to study their Pharmacokinetics properties of the resulted oral drug delivery systems.

ASSOCIATED CONTENT

Supporting Information.

This material is available free of charge via the Internet at <http://pubs.acs.org>.

AUTHOR INFORMATION

Corresponding Author

* Ahmed Al-Yasari^{1,2}

¹Department of Chemistry, College of Science, University of Kerbala, Al-Ferahe, Kerbala, Iraq

² School of Chemistry, University of East Anglia, Norwich Research Park, Norwich, NR7 4TJ, UK

a.alyasari@uokerbala.edu; a.al-yasari@uea.ac.uk.

AUTHOR CONTRIBUTIONS

The manuscript was written through contributions of all authors.

ACKNOWLEDGMENT

We gratefully acknowledge the University of East Anglia for providing support to the use of the ADA supercomputer's computational resources. Al-Yasari particularly thanks the University of East Anglia School of Chemistry for providing the visiting status research position. Dr Joseph Wright is also acknowledged by A. Al-Yasari for his valuable support.

References:

- (1) Stupp, R.; Gander, M.; Leyvraz, S.; Newlands, E. Current and Future Developments in the Use of Temozolomide for the Treatment of Brain Tumours. *Lancet Oncol.* **2001**, *2* (9), 552–560. [https://doi.org/10.1016/S1470-2045\(01\)00489-2](https://doi.org/10.1016/S1470-2045(01)00489-2).
- (2) Newlands, E. S.; Stevens, M. F. G.; Wedge, S. R.; Wheelhouse, R. T.; Brock, C. Temozolomide: A Review of Its Discovery, Chemical Properties, Pre-Clinical Development and Clinical Trials. *Cancer Treat. Rev.* **1997**, *23* (1), 35–61. [https://doi.org/10.1016/S0305-7372\(97\)90019-0](https://doi.org/10.1016/S0305-7372(97)90019-0).
- (3) Stevens, M. F. G.; Newlands, E. S. From Triazines and Triazenes to Temozolomide. *Eur. J. Cancer* **1993**, *29* (7), 1045–1047. [https://doi.org/10.1016/S0959-8049\(05\)80221-7](https://doi.org/10.1016/S0959-8049(05)80221-7).
- (4) Emamgholizadeh Minaei, S.; Khoei, S.; Khoei, S.; karimi, M. R. Tri-Block Copolymer Nanoparticles Modified with Folic Acid for Temozolomide Delivery in Glioblastoma. *Int. J. Biochem. Cell Biol.* **2019**, *108*, 72–83. <https://doi.org/10.1016/j.biocel.2019.01.010>.
- (5) Ramalho, M. J.; Coelho, M. A. N.; Pereira, M. C. Chapter 18 - Nanocarriers for the Delivery of Temozolomide in the Treatment of Glioblastoma: A Review. In *Design and Development of New Nanocarriers*; Grumezescu, A. M., Ed.; William Andrew Publishing, 2018; pp 687–722. <https://doi.org/10.1016/B978-0-12-813627-0.00018-1>.

- (6) Song, Y.-F.; Tsunashima, R. Recent Advances on Polyoxometalate-Based Molecular and Composite Materials. *Chem. Soc. Rev.* **2012**, *41* (22), 7384–7402. <https://doi.org/10.1039/C2CS35143A>.
- (7) Izzet, G.; Volatron, F.; Proust, A. Tailor-Made Covalent Organic-Inorganic Polyoxometalate Hybrids: Versatile Platforms for the Elaboration of Functional Molecular Architectures. *Chem. Rec.* **2017**, *17* (2), 250–266. <https://doi.org/10.1002/tcr.201600092>.
- (8) Bijelic, A.; Aureliano, M.; Rompel, A. Polyoxometalates as Potential Next-Generation Metallo-drugs in the Combat Against Cancer. *Angew. Chemie Int. Ed.* **2019**, *58* (10), 2980–2999. <https://doi.org/10.1002/anie.201803868>.
- (9) Gao, Y.; Choudhari, M.; Such, G. K.; Ritchie, C. Polyoxometalates as Chemically and Structurally Versatile Components in Self-Assembled Materials. *Chem. Sci.* **2022**, *13* (9), 2510–2527. <https://doi.org/10.1039/D1SC05879G>.
- (10) Petrovskii, S. K.; Moors, M.; Schmitz, S.; Grachova, E. V.; Monakhov, K. Y. Increasing the Redox Switching Capacity of Lindqvist-Type Hexavanadates by Organogold Post-Functionalisation. *Chem. Commun.* **2023**, *59* (62), 9517–9520. <https://doi.org/10.1039/D3CC02511J>.
- (11) Amin, S. S.; Jones, K. D.; Kibler, A. J.; Damian, H. A.; Cameron, J. M.; Butler, K. S.; Argent, S. P.; Winslow, M.; Robinson, D.; Mitchell, N. J.; et al. Diphosphoryl-functionalized Polyoxometalates: Structurally and Electronically Tunable Hybrid Molecular Materials. *Angew. Chemie* **2023**, *135* (23). <https://doi.org/10.1002/ange.202302446>.
- (12) Al-Yasari, A.; Alesary, H.F.; Alghurabi, H.; Ali Alali, M.M.M.; Ahmed, L.M.; Alasadi, R. Methotrexate PH-Responsive Release from Nanostructures of Dopamine and Polyoxometalate. *Biochem. Cell. Arch.* **2019**, *19* (2), 3675–3680. <https://doi.org/10.35124/bca.2019.19.2.3675>.
- (13) Li, H.; Jia, Y.; Wang, A.; Cui, W.; Ma, H.; Feng, X.; Li, J. Self-Assembly of Hierarchical Nanostructures from Dopamine and Polyoxometalate for Oral Drug Delivery. *Chem. – A Eur. J.* **2014**, *20* (2), 499–504. <https://doi.org/10.1002/chem.201302660>.
- (14) Ahmed, L.; Ali, S.; Ali, M. Hybrid Phosphotungstic Acid -Dopamine (PTA-DA) Like-Flower Nanostructure Synthesis as a Furosemide Drug Delivery System and Kinetic Study of Drug Releasing. *Egypt. J. Chem.* **2021**, 0–0. <https://doi.org/10.21608/ejchem.2021.75210.3692>.
- (15) Geisberger, G.; Paulus, S.; Gyenge, E. B.; Maake, C.; Patzke, G. R. Targeted Delivery of Polyoxometalate Nanocomposites. *Small* **2011**, *7* (19), 2808–2814. <https://doi.org/10.1002/smll.201101264>.
- (16) Cameron, J. M.; Guillemot, G.; Galambos, T.; Amin, S. S.; Hampson, E.; Mall Haidaraly, K.; Newton, G. N.; Izzet, G. Supramolecular Assemblies of Organo-Functionalised Hybrid Polyoxometalates: From Functional Building Blocks to Hierarchical Nanomaterials. *Chem. Soc. Rev.* **2022**, *51* (1), 293–328. <https://doi.org/10.1039/D1CS00832C>.
- (17) Wang, X.; Wei, S.; Zhao, C.; Li, X.; Jin, J.; Shi, X.; Su, Z.; Li, J.; Wang, J. Promising Application of Polyoxometalates in the Treatment of Cancer, Infectious Diseases and

Alzheimer's Disease. *JBIC J. Biol. Inorg. Chem.* **2022**, *27* (4–5), 405–419. <https://doi.org/10.1007/s00775-022-01942-7>.

(18) Black, F. A.; Jacquart, A.; Toupalas, G.; Alves, S.; Proust, A.; Clark, I. P.; Gibson, E. A.; Izzet, G. Rapid Photoinduced Charge Injection into Covalent Polyoxometalate-Bodipy Conjugates. *Chem. Sci.* **2018**. <https://doi.org/10.1039/c8sc00862k>.

(19) El Moll, H.; Black, F. A.; Wood, C. J.; Al-Yasari, A.; Reddy Marri, A.; Sazanovich, I. V.; Gibson, E. A.; Fielden, J. Increasing P-Type Dye Sensitised Solar Cell Photovoltages Using Polyoxometalates. *Phys. Chem. Chem. Phys.* **2017**, *19* (29), 18831–18835. <https://doi.org/10.1039/C7CP01558E>.